

# Spatiotemporal expression and inhibition of prolyl oligopeptidase contradict its involvement in key pathologic mechanisms of kainic acid–induced temporal lobe epilepsy in rats

Idrish Ali<sup>1</sup> | Annemie Van Eetveldt<sup>1</sup> | Roos Van Elzen<sup>2</sup> | Tom Kalathil Raju<sup>2</sup> |  
Pieter Van Der Veken<sup>3</sup> | Anne-Marie Lambeir<sup>2</sup> | Stefanie Dedeurwaerdere<sup>4</sup>

<sup>1</sup>Department of Translational Neurosciences, University of Antwerp, Wilrijk, Belgium

<sup>2</sup>Laboratory of Medical Biochemistry, University of Antwerp, Wilrijk, Belgium

<sup>3</sup>Laboratory of Medicinal Chemistry, University of Antwerp, Wilrijk, Belgium

<sup>4</sup>Laboratory of Experimental Hematology, Vaxinfectio, University of Antwerp, Antwerp, Belgium

## Correspondence

Anne-Marie Lambeir, Laboratory of Medical Biochemistry, Department of Pharmaceutical Sciences, University of Antwerp, Wilrijk, Belgium.  
Email: anne-marie.lambeir@uantwerpen.be

## Present Address

Idrish Ali, Department of Medicine, University of Melbourne, Melbourne, Australia

Stefanie Dedeurwaerdere, UCB Pharma, Braine-l'Alleud, Belgium

## Funding information

Fonds Wetenschappelijk Onderzoek, Grant/Award Number: G038515N

## Summary

**Objective:** Prolyl oligopeptidase (PREP) has been implicated in neuroinflammatory processes and neuroplasticity and has been suggested as a target for the treatment of neurodegenerative disease. The aim of this investigation was to explore the involvement of PREP in the neuropathologic mechanisms relevant to temporal lobe epilepsy (TLE) using a PREP inhibitor in a well-established rat model.

**Methods:** PREP activity and expression was studied in Sprague-Dawley rats 2 and 12 weeks following kainic acid–induced status epilepticus (KASE). Continuous video-electroencephalography monitoring was performed for 2 weeks in the 12-week cohort to identify a relationship of PREP expression/activity with epileptic seizures. In addition, the animals included in the 2-week time point were treated with a specific inhibitor of PREP, KYP-2047, or saline continuously, starting immediately after SE. PREP activity and its expression were analyzed in rat brain by using enzyme kinetics and western blot. In addition, markers for microglial activation, astrogliosis, cell loss, and cell proliferation were evaluated.

**Results:** Enzymatic activity of PREP was unchanged following induction of SE after 2 and 12 weeks in rats. PREP activity in epileptic rats did not relate to the number of seizures/day at the 12-week time point. Moreover, continuous inhibition of PREP for 2 weeks after KASE did not alter the SE-mediated neuroinflammatory response, cell loss, or cell proliferation in the hippocampal subgranule zone measured at the 2-week time point.

**Significance:** PREP inhibition does not affect key pathologic mechanisms, including activation of glial cells, cell loss, and neural progenitor cell proliferation, in this KASE model of TLE. The results do not support a direct role of PREP in seizure burden during the chronic epilepsy period in this model.

## KEY WORDS

inflammation, prolyl oligopeptidase, temporal lobe epilepsy

## 1 | INTRODUCTION

Epilepsy is a devastating neurologic disorder that affects around 65 million people worldwide. Current antiepileptic drugs are only symptomatic and around one-third of patients do not respond to treatment, highlighting the need to explore new therapies. Many studies have uncovered a connection between epilepsy and neuroinflammation. Brain inflammation is a key mechanism for repair after an insult, and it plays an important role in the pathology of various types of epilepsy.<sup>1,2</sup> A proinflammatory response can contribute to cell death,<sup>3,4</sup> network excitability,<sup>5,6</sup> and synaptic reorganization.<sup>7,8</sup> It has been shown that there is a positive correlation between the expression of translocator protein (TSPO), a biomarker of neuroinflammation, and seizure burden in a rat model of temporal lobe epilepsy (TLE), emphasizing the role of inflammation in epilepsy.<sup>9,10</sup> Moreover, antiinflammatory approaches during epileptogenesis in animal models of acquired epilepsy can affect seizure development.<sup>2,11,12</sup>

Prolyl oligopeptidase (PREP), a proline-specific endopeptidase, has been proposed to be involved in neurodegeneration, cell proliferation, differentiation, and neuroinflammation.<sup>13-15</sup> The proposed underlying mechanisms include modification of neuropeptides and alteration of inositol triphosphate, an intracellular signaling molecule, to control gene expression, although no clear role has been established to date. In the healthy brain, PREP is present mostly in neurons: in the cytoplasm, around the nucleus along the microtubules, and at the tips of the neurites.<sup>16</sup> A strong neuroinflammatory condition increases PREP activity and expression in astrocytes and microglia in mouse brain<sup>13</sup> as well as in the astrocytes from resected brain tissue from patients with Parkinson or Alzheimer disease.<sup>17</sup> PREP expression is also upregulated in glial cells after activation with lipopolysaccharide (LPS)<sup>13</sup> and is found to be neurotoxic to co-cultured neuronal cells, an effect that was reversed by PREP inhibitors.<sup>18</sup> Accordingly, administration of antiinflammatory agents in a neuroinflammatory environment restores PREP expression to normal levels.<sup>19</sup> PREP has also been reported to generate peptides that assist chemotaxis in blood neutrophils<sup>20</sup> and may promote their transmigration in epileptic brain.<sup>21</sup>

In addition, PREP<sup>-/-</sup> mice are reported to have defects in growth cone formation<sup>22</sup> and display decreased hippocampal synaptic plasticity with impaired learning and memory.<sup>23,24</sup> PREP overexpression has been shown to reduce the levels of polysialylated neural cell adhesion molecule (PSA-NCAM), whereas in PREP-negative mice, PSA-NCAM level was increased.<sup>25</sup> PSA-NCAM in turn plays pivotal roles in neurogenesis and plasticity.<sup>26</sup> Loss of PSA-NCAM by upregulated PREP could mediate enhanced acute excitability relevant to epileptogenesis.<sup>27</sup>

### Key Points

- PREP activity did not change in a model of TLE
- Inhibiting PREP activity did not alter neuroinflammation or neuronal cell counts
- PREP activity did not correlate to seizures in the chronic epilepsy period
- PREP may not be involved in pathologic mechanisms of TLE

Abnormal synaptic plasticity with aberrant neurogenesis and neuroinflammation are pathophysiologic hallmarks of TLE. Based on the background that PREP is related to increased neuroinflammation and synaptic plasticity, we hypothesized that PREP inhibition may affect key pathologic mechanisms related to epilepsy and may provide a novel target against epileptogenesis. A previous study has shown alterations in PREP activity in the hours following pentylenetetrazol (PTZ)-induced seizures in rats.<sup>28</sup> This study showed a reduced PREP activity acutely 0.5-3 hours after PTZ-induced seizures.

PREP activity measurements in chronic models of TLE or effects of modulating PREP on pathologic outcomes after epileptogenic injury are yet to be investigated. Therefore, we investigated whether PREP can be a novel target that may provide an antiepileptogenic intervention against TLE. PREP expression was evaluated in rat brain at 2 weeks, the time point representing the highest microglia and astrocyte activation in our previous studies, as well as at 3 months, representing chronic epilepsy in a kainic acid-induced status epilepticus (KASE) model. In addition, we evaluated the effects of continuous inhibition of PREP activity on neurodegeneration, neuroinflammation, and hippocampal subgranule zone-cell proliferation by the selective PREP inhibitor KYP-2047, for 2 weeks immediately after SE.

## 2 | MATERIALS & METHODS

### 2.1 | Animals

Seven-week-old male Sprague-Dawley rats (Harlan Laboratories B.V., The Netherlands) were single housed under a 12-hour light/dark cycle, in a temperature- and humidity-controlled environment. Food and water were provided ad libitum. Animals were treated according to the guidelines from the European Ethics Committee (decree 86/609/CEE) and the Animal Welfare Act (7 USC 2131). All animal experiments were approved (ECD 2014-74) by the ethical committee of the University of Antwerp (Belgium).

## 2.2 | Study design

A total of 58 rats were used for the study. Thirty-six rats were used for evaluating PREP activity and investigating the effects of PREP inhibition on neuroinflammation at early periods of disease onset (14-day time point). Of these, 30 rats were subjected to KASE and were randomly assigned to either the KYP-2047 or vehicle-treated group. Osmotic pumps with a selective inhibitor of PREP,<sup>29</sup> KYP-2047 ( $n = 15$ , 34 mg/kg/day) or saline ( $n = 15$ ) were implanted 4 hours after KASE (see section 2.4). After pump implantation, the animals received a loading dose of vehicle or KYP-2047 (17 mg/kg) subcutaneously followed by sustained delivery (34 mg/kg/day). Another 6 animals were included as healthy controls for histologic comparisons. Initial pilot experiments were performed to determine the dose of KYP-2047 and target engagement in brain and plasma.

Another 22 rats were included for evaluating PREP activity during the chronic epilepsy period (3 months post-KASE induction). Nine animals underwent SE induction while 13 rats served as healthy control animals. These animals also underwent continuous video-electroencephalography recordings (vEEG) for 2 weeks before they were killed.

## 2.3 | KYP-2047 dose determination

To determine the dose of KYP-2047, the level of PREP inhibition was measured in a pilot experiment following single-dose and continuous administration of KYP-2047 in rats. A 17 mg/kg dose of KYP-2047 was shown to be effective before in terms of inhibiting PREP activity in the brain.<sup>30</sup> We tested PREP activity in plasma after a single injection of KYP-2047 in rats ( $n = 4$ ) at 5, 10, 30 minutes, and at 1, 2, 5, and 24 hours. In addition, brains were collected after a single injection of KYP-2047 at 15 minutes, and at 1, 5, and 15 hours to measure PREP inhibition in brain tissue ( $n = 4$  for each time point). For chronic PREP inhibition, 34 mg/kg/day ( $n = 3$  for control rats) and 51 mg/kg/day of KYP-2047 ( $n = 3$  each for control and KASE rats) were administered for 1 week using an osmotic pump, after giving a loading dose of 17 mg/kg subcutaneously. Blood samples were collected at 24, 48, and 72 hours and brain was collected at 1 week of treatment.

## 2.4 | Induction of SE and pump implantation

A modified protocol based on the multiple low-dose kainic acid injection protocol of Hellier et al.<sup>31</sup> was used for the induction of KASE as described previously.<sup>10</sup> At SE induction, the rats were aged 7.5 weeks with an average weight of  $226 \pm 4.42$  (SD) g. The animals of the vehicle, KASE, and treated KASE group received subcutaneously an initial dose

of 5 mg/kg KA (A.G. Scientific Inc.), which was repeated every hour until the animals went into SE. The naive control animals received saline injections only. Osmotic pumps with drug or vehicle were implanted beneath the subcutaneous tissue on the back of the rats under isoflurane anesthesia 4 hours after KASE, as described previously.<sup>9</sup> An additional subcutaneous injection of saline or KYP-2047 (loading dose of 17 mg/kg) was administered immediately after pump implantation. The osmotic pumps (Alzet, 2 mL delivery in 2 weeks; Charles River, France) delivered KYP-2047 (34 mg/kg/day) or saline for 2 weeks continuously.

## 2.5 | vEEG monitoring and spontaneous recurrent seizure evaluation

The animals from the 12-week time point underwent vEEG recording for 2 weeks before being killed. The electrodes were implanted 2 weeks before the commencement of recordings as described previously.<sup>32</sup> The animals were connected to the digital EEG acquisition system (Ponemah P3 Plus; Data Sciences International) through a cable system with commutator for continuous video monitoring.<sup>10</sup> The analysis was performed manually by an observer blinded to the animal ID using Neuroscore 3.0 (Data Sciences International). The identification of the spontaneous recurrent seizures (SRS) was performed as described.<sup>9</sup>

## 2.6 | Tissue processing

At the end of experiments, all animals were killed by rapid decapitation. Brains were immediately dissected and fresh frozen in 2-methylbutane at  $-35^{\circ}\text{C}$  and preserved at  $-80^{\circ}\text{C}$  until sectioning. For PREP inhibition experiments, the brain was cut into 2 hemispheres and the left hemisphere was used for western blot and PREP activity measurements, while the right hemisphere was used for histologic evaluations: serial coronal sections ( $20\ \mu\text{m}$ ) were collected at  $-3.24$  mm from bregma (dorsal hippocampus).<sup>33</sup> Slides with sections were postfixed in 4% paraformaldehyde at room temperature for 10 minutes for immunohistochemistry.

## 2.7 | Immunohistochemistry

Immunohistochemical staining was performed to assess neuronal cell loss (NeuN), cell proliferation (Ki67), and the abundance of microglia/macrophages (OX-42), phagocytic cells (CD-68), and astrocytes (Glial fibrillary acidic protein, GFAP). The protocols for NeuN, OX-42, CD-68, and GFAP staining were published previously.<sup>9,10,34-37</sup> The antibodies used in the immunohistochemical experiments are listed in Table 1.

For Ki67 staining, the sections were fixed with 4% paraformaldehyde for 10 minutes followed by incubation with

**TABLE 1** Summary of antibodies used for immunohistochemistry

Target	Marker	Antibody	Type
Primary antibodies			
Neuronal cells	NeuN	Merck Millipore, MAB377, 1:2000	mouse IgG
Microglia/macrophages	OX-42	AbDserotec, MCA275R, 1:1000	mouse IgG
Phagocytic cells	CD-68	AbDserotec, MCA341GA, 1:200	Mouse IgG
Astrocytes	GFAP	Dako, Z0334, 1:1000	Rabbit
Cell proliferation	Ki67	Abcam, ab16667, 1:400	Rabbit
Secondary antibodies			
Jackson ImmunoResearch, peroxidase-conjugated goat anti-rabbit IgG Fab2: 111-065-006 (used with GFAP and Ki67), 1:500 and 1:200, respectively			
Jackson ImmunoResearch, peroxidase-conjugated donkey anti mouse IgG: 715-035-150, (used with OX-42, NeuN, and CD-68), 1:500			

3% hydrogen peroxide for 5 minutes. Nonspecific binding was blocked using 0.5% Triton X-100 and 5% normal goat serum (NGS) in phosphate-buffered saline (PBS) for 1 hour. Subsequently the sections were incubated overnight at room temperature with a primary monoclonal antibody solution of rabbit anti-Ki67 (1:400; Abcam, UK) in blocking buffer (1% NGS). The sections were then washed and incubated for 1 hour with peroxidase-conjugated goat anti-rabbit secondary antibody (1:200; Jackson ImmunoResearch Lab Inc.) in blocking buffer. Finally, the sections were exposed to diaminobenzidine for 10 minutes.

The region of interest (ROI) was manually delineated based on the morphology of the rat brain. ROI included the entire hippocampal cornu ammonis (CA)1, CA3, CA4, hilar sub-regions, and piriform cortex (PC). The evaluations were done by an investigator blinded to treatment on triplicate (consecutive) sections of which the mean score was used for statistical analysis. The specific details for the different evaluation methods are outlined below.<sup>3,10,34-37</sup>

For Ox-42 staining, images of ROIs were taken at 4× magnification with an AxioCam Erc5s (ZEISS, Germany) and converted into 8-bit images in ImageJ. Using ImageJ, an intensity threshold was set visually to detect all stained cells above background. The same threshold was applied for all animals. The full area of the ROI was manually delineated in ImageJ blinded for the treatment group. ImageJ automatically calculates the percentage of the delineated area (ROI) with a gray value above the threshold (% area), representing the abundance of microglia in ROI due to their proliferation and activation.

For NeuN staining, images of ROIs were taken at 4× magnification with an AxioCam Erc5s (ZEISS, Germany) and converted into 8-bit images in ImageJ. Using ImageJ, an intensity threshold was set visually to detect all stained cells above background. The same threshold was applied for all

animals. The full area of the ROI was manually delineated in ImageJ blinded for the treatment group. ImageJ automatically calculates the number of NeuN-positive cells per ROI surface (cell count/mm<sup>2</sup>).

For CD-68 and GFAP staining, cells were counted manually under the microscope (Olympus C × 31) at 40× magnification in the ROI. ROIs were delineated for each hippocampal subregion and piriform cortex. The number of positive cells was counted and scored along a semi-quantitative scale. The number of CD-68<sup>+</sup> cells was scored between 0 and 5, with a score of 0 indicating no CD-68<sup>+</sup> cells; 1, 0-20 cells; 2, 21-40 cells; 3, 41-60 cells; 4, 61-80 cells, and 5, >80 cells in the examined area. The number of GFAP-positive cells was scored between 0 and 5, with 0 (0-20 cells), 1 (21-40 cells), 2 (41-60 cells), and 3 (61-80 cells including mutually overlapping cells) to 4 (81-100 including mutually overlapping cells), and 5 (>100 cells).

Ki67-positive cells were also counted in the subgranular zone (SGZ), the zone comprising the innermost row of cells in the granule cell layer (GCL) along with 2-cell-diameter thick regions at the GCL/hilar border.<sup>3</sup> The cells were counted in 3 sections and the average number of cells per section was recorded.

## 2.8 | TSPO autoradiography

TSPO expression was determined by in vitro autoradiography with a specific radiolabeled ligand for TSPO, <sup>3</sup>H-PK11195 (PerkinElmer).<sup>10</sup> <sup>3</sup>H-PK11195 total and nonspecific binding was quantitatively measured in the ROIs.

## 2.9 | PREP activity in blood and brain tissue

For the preparation of tissue homogenates, 20 mg of N<sub>2</sub>-pulverized rat brain were suspended in 250 μL PREP lysis

buffer (0.1 mol/L Tris-HCl pH 7.4, 1 mmol/L EDTA, 1% octyl glucoside, 50 µg/mL aprotinin, 5 mmol/L DTT). The samples were left on ice for 1 hour and centrifuged at 4°C at 12 000 g for 15 minutes. PREP activities were measured kinetically on the clarified supernatants using Z-Gly-Pro-pNA (Bachem, Bubendorf, Switzerland) (250 µmol/L, 5% dimethyl sulfoxide [DMSO]) in 0.1 mol/L Tris-HCl pH 7.4, 1 mmol/L EDTA, 3 mM DTT as described.<sup>38</sup>

For determining PREP activity in rat plasma, the fluorescent substrate Z-Gly-Pro-AMC (Bachem, Bubendorf, Switzerland; 250 µmol/L in 5% DMSO) was used. The activities were determined kinetically for 60 minutes at 37°C by measuring the velocity of AMC release ( $\lambda_{\text{ex}} = 380 \text{ nm}$ ,  $\lambda_{\text{em}} = 460 \text{ nm}$ ). Fluorescence intensity was related to an AMC standard curve in the same buffer. One unit of activity was defined as the amount of enzyme catalyzing the conversion of 1 µmol of substrate in 1 minute under reaction conditions. All activities were normalized to the protein content in the lysates as determined in a Bradford assay.

## 2.10 | Western blotting

The rat brain homogenates were diluted in Laemmli sample buffer (2×) and heat denatured before loading onto a 10% sodium dodecyl sulfate polyacrylamide gel. After complete separation, the proteins were transferred to a nitrocellulose membrane (Bio-Rad, Hercules, California) in 90 minutes at 250 mA in a wet electroblot chamber. Nonspecific binding sites on the membranes were blocked by incubation in 5% bovine serum albumin (BSA) in 50 mmol/L Tris-HCl pH 7.5, 150 mmol/L NaCl (TBS) overnight at 4°C. Then the membranes were incubated with either anti-PREP antibody (rabbit polyclonal antibody described by Julku et al 2018, 1:1000 dilution<sup>39</sup>) or anti-beta-Actin as loading control (A1978, 1:5000 dilution, Sigma-Aldrich, Overijse, Belgium) in 5%

BSA in TBS. Next, the membranes were incubated, respectively, with HRP-goat anti-rabbit (656120), or HRP-rabbit anti-mouse (A10677) 1:5000 dilution, (LifeTechnologies, Ghent, Belgium), for 1 hour at room temperature. The immune reaction was detected using the SuperSignal West Femto substrate kit (Thermo Scientific, Erembodegem, Belgium). Images were acquired with an OptiGo-750 (Isogen Life Sciences, De Meern, The Netherlands) and the densitometry was performed with ImageJ.

## 2.11 | Statistical analysis

The Kolmogorov-Smirnov test showed that not all data sets were normally distributed, and therefore nonparametric tests were used for the analysis. For the 12-week time point, PREP activity and expression were compared between KASE and the control group using the Mann-Whitney *U* test. For PREP inhibition experiments, the comparison between the 3 groups—naive control, KASE animals treated with KYP-2049, or vehicle—was performed using the Kruskal-Wallis test with a post hoc Dunn's multiple comparison test. All analyses were done using GraphPad Prism 6 software (GraphPad) or R (RStudio) software. Statistical significance was set at  $P \leq 0.05$ .

## 3 | RESULTS

### 3.1 | KYP-2047 inhibits the activity but not the expression of PREP

A bolus dose of 17 mg/kg KYP-2047 was consistently found to inhibit PREP activity by around 60% of control values in both blood and brain within the first hour of injection (Figure 1A). A bolus dose (17 mg/kg) followed by a sustained administration of KYP-2047 with an osmotic pump

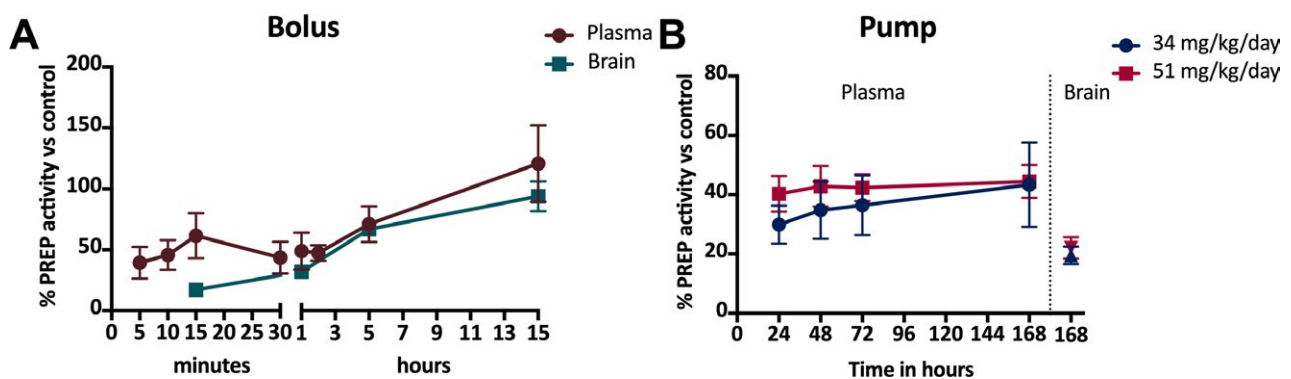


**FIGURE 1** Prolyl oligopeptidase (PREP) enzymatic activity time course after administration of (A) a bolus dose of KYP-2047 (17 mg/kg;  $n = 4$  for all time points except for 1 & 5 h where  $n = 8$  rats were used) and (B) a bolus dose followed by a pump implantation delivering KYP-2047 either 34 mg/kg/day ( $n = 5$ ) or 51 mg/kg ( $n = 3$ ). Sustained inhibition in PREP activity (60%-70% inhibition in plasma and 80% in brain) was observed following 1 week of KYP-2047 administration, which was similar to the inhibition observed following a single dose of inhibitor. No differences in PREP inhibition was observed between 34 and 51 mg/kg/day; therefore, the lower dose was used for the study. Both 51 and 34 mg/kg/day dose were well tolerated and no adverse behavioral events were observed. Data are represented as mean  $\pm$  SD

(34 mg/kg/day or 51 mg/kg/day) maintained PREP inhibition at the initial level (Figure 1B). Therefore, we chose to use a bolus of 17 mg/kg followed by a 34 mg/kg/day administration of KYP-2047 via an osmotic pump to chronically inhibit PREP activity. Both 34 and 51 mg/kg/day doses were well tolerated without any adverse behavior events.

The enzymatic activity of PREP was measured in brain and plasma of KASE rats (both after vehicle or KYP-2047 administration) in comparison with the naive control rats. The activity of PREP was unchanged 2 weeks following the induction of SE, for vehicle-treated KASE rats compared to naive controls (Figure 2A). PREP activity was also measured 12 weeks after KASE. This period represents the chronic epilepsy period during which KASE rats experience spontaneous recurrent epileptic seizures. The PREP activity in KASE rats was comparable to that of age-matched naive controls (Figure 2B). Measured together in a single experiment to avoid interexperiment

variation, PREP activity for the 2-week and 12-week time points remained the same during the course of epilepsy progression.

PREP inhibition in KYP-2047-treated KASE rats after 2 weeks was ~85% in brain (Figure 2A) and ~40% in plasma (Figure 2C) when compared to the vehicle-treated KASE rats. The residual activity in plasma can be attributed to the presence of fibroblast-activating protein (FAP) in plasma but not in brain homogenates. FAP converts the substrate used in the enzymatic assay but is not inhibited by KYP-2047.<sup>40</sup> The amount of immunoreactive PREP in whole-brain homogenates was significantly reduced in KASE rats after 2 weeks when compared to naive controls (Figure 2D,E). Treatment of KASE rats with KYP-2047 for 2 weeks did not alter PREP expression compared to vehicle-treated KASE rats. The expression level of PREP in whole brain homogenate at the 12-week time point was not altered compared to the naive controls (Figure 2F).

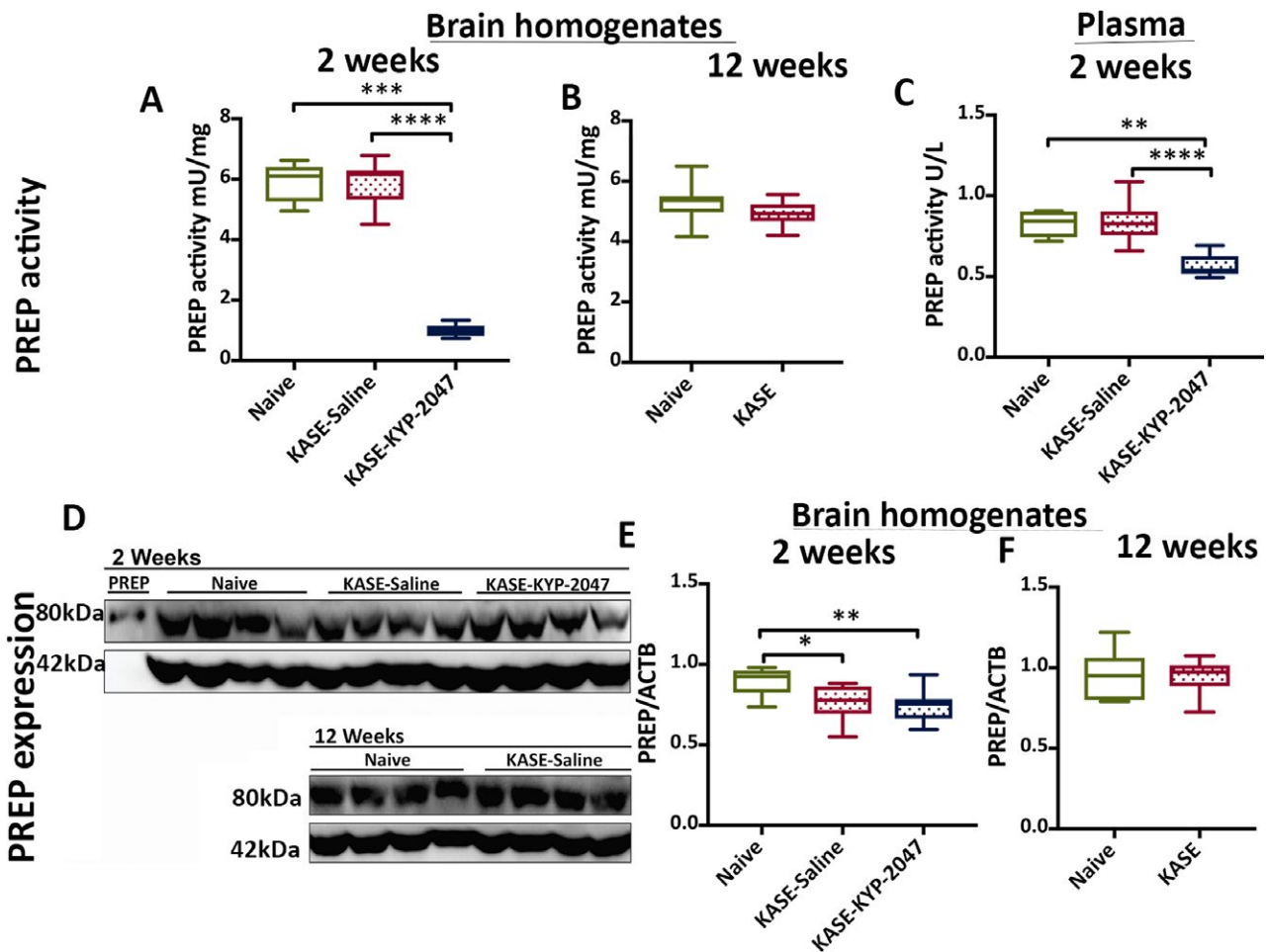


**FIGURE 2** Prolyl oligopeptidase (PREP) specific activity decreased but the expression of PREP remained the same in KYP-2047-treated KASE rats when compared to saline-treated KASE rats. PREP activity measured in brain lysates at (A) 2-week and (B) 12-week time points using the substrate Z-Gly-Pro-pNA. C, PREP activity measured in plasma using the fluorogenic substrate Z-Gly-Pro-AMC after 2 weeks of KYP-2047 administration. D, Representative western blot of PREP in brain lysates at 2 and 12 weeks after KASE induction. Beta-actin (ACTB) was used as a loading control. Quantification of PREP expression in brain lysates at (E) 2 weeks and (F) 12 weeks after KASE induction. Data are represented as median  $\pm$  interquartile ranges (\* $P < 0.05$ , \*\*\* $P < 0.001$ )

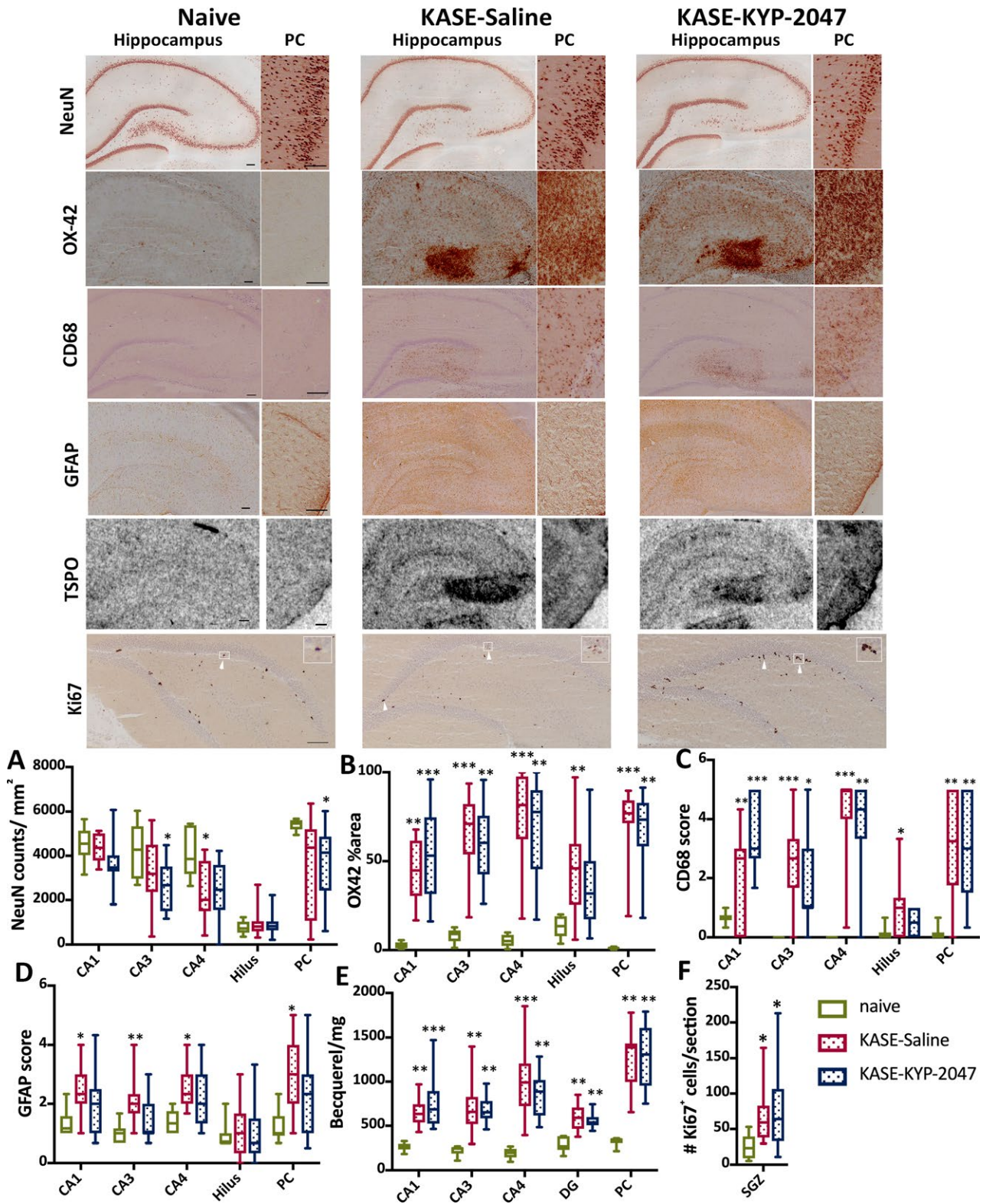


**FIGURE 3** Cell loss, neuroinflammation, and neurogenesis remained unaltered following KYP-2047 treatment. Representative images and graphs quantifying (A) NeuN cell density; (B) OX-42% area; (C) CD-68 scores; (D) GFAP scores; and (E) TSPO specific binding in hippocampal CA1, CA3, CA4, hilar subregions, and piriform cortex (PC). F, Number of Ki67-positive cells per section in the subgranular zone of the hippocampus. White arrow head and inset in representative images show zoomed images. Data are represented as median  $\pm$  interquartile ranges (\* $P < 0.05$ , \*\* $P < 0.01$ , \*\*\* $P < 0.001$ ;  $n = 15$ /group for saline and KYP-2047-treated rats and  $n = 6$  for naive rats). All scale bars in representative images are 200  $\mu$ m

### 3.2 | SE-mediated neuronal loss, neuroinflammation, and hippocampal subgranule zone-cell proliferation remained unchanged following PREP inhibition

The effect of PREP inhibition on cell death was evaluated in SE rats after 2 weeks by NeuN staining (Figure 3A). Continuous administration of PREP inhibitor KYP-2047 did not affect NeuN cell counts in any of the evaluated regions compared to the saline-treated KASE animals (Figure 3A). Second, the effect of 2-week continuous PREP inhibition on neuroinflammation was evaluated using OX-42 (Figure 3B) and CD-68 (Figure 3C) staining, which are markers of activated and phagocytic microglia, respectively. KASE rats displayed strong neuroinflammation, as evident by a significant increase in all hippocampal subregions and piriform cortex for the OX-42% area and CD-68 scores, when compared to the naive animals. Administration of KYP-2047 in SE rats did not alter the OX-42% area or the CD-68 scores when compared to saline-treated SE rats. Accordingly, the OX-42% area and CD-68 scores remained significantly higher in both SE groups compared to the control animals, except in the dentate hilus (DH) region where it did not reach statistical significance. Similarly, GFAP scores were significantly higher in all evaluated regions of saline-treated SE rats when compared to naive rats, suggesting a strong astrogliosis following SE induction (Figure 3D). However, administration of KYP-2047 did not alter GFAP scores following SE induction. These results were confirmed by measuring the levels of TSPO, an imaging biomarker of inflammation (Figure 3E). There was a significant increase in TSPO binding in KASE rats (both saline and KYP-2047 treated) when compared to the naive rats. No effect of KYP-2047 administration was observed in comparison with the saline-treated rats (Figure 3E). Finally, we quantified the number of Ki67-positive cells within the subgranule zone of the hippocampus, an area that is known to support neural stem cells and display increased neural cell proliferation following an epileptic seizure. There was a significant increase in the Ki67-positive cells in rats that underwent SE compared to naive rats, suggesting an increased proliferation in these animals (Figure 3F). However, KYP-2047 administration did not alter the number of Ki67-positive cells.

### 3.3 | PREP activity during chronic epilepsy was not associated with spontaneous recurrent seizures

Continuous vEEG monitoring of animals for 2 weeks during the chronic epilepsy period revealed that all the animals had developed spontaneous epileptic seizures by this period (median: 6.61 seizures/day [mean: 11.5 seizures/day], with a maximum: 37.4 seizures/day and minimum: 0.65 seizures/

day) with predominantly convulsive seizures (S3-S5 according to the Racine scale). To understand whether PREP activity is related to the seizure outcome during the chronic epilepsy period, we performed correlations of PREP activity with the average number of seizures/day and average number of severe convulsive seizures/day in rats that underwent vEEG monitoring. No significant correlations were observed with respect to the average number of seizures per day ( $r = 0.2$ ;  $P = 0.6$ ) or convulsive seizures/day ( $r = 0.05$ ;  $P = 0.9$ ) with PREP activity during the chronic epilepsy period.

## 4 | DISCUSSION

In the current study, we evaluated the effect of PREP inhibition on the pathogenesis of temporal lobe epilepsy. Continuous administration of a specific inhibitor of PREP strongly reduced the PREP-specific activity at 2 weeks after KASE without a proportional change in its expression levels, as expected for an active-site inhibitor. Although PREP-specific activity was not significantly altered in KASE animals at both time points, a slight but significant reduction in PREP expression was observed at the 2-week time point. Inhibiting PREP activity for 2 weeks immediately after SE did not modify microglia and astrocyte activation, neuronal counts, or hippocampal subgranule zone-cell proliferation. Furthermore, PREP activity during chronic epilepsy did not relate to the seizure burden in epileptic rats.

Based on the literature cited in the Introduction, we expected an increased expression/activity of PREP in a strong inflammatory environment. However, PREP activity was not altered in the overall brain homogenate, despite a persistent increase in TSPO binding, activated microglia, and reactive astrocytes observed in KASE animals at both the 2-week and 12-week time points. Instead, there was reduced PREP expression at the 2-week time point after KASE. Of interest, using PTZ to induce seizures, Ahmed and coworkers observed a transient decrease in PREP activity in the hippocampus and frontal cortex that normalized within 1 day. In other brain regions, PREP activity was not statistically changed.<sup>28</sup> Apart from the differences in mode of action between the 2 chemical convulsants, the major difference between the PTZ study and this one is that the former is an acute model, whereas the post-KA induced SE (KASE) model is a chronic model. These short-term changes may not be picked up at the 2-week time point or may be obscured by measuring activity in a total brain homogenate. However, both models are characterized by activation of microglia associated with an increase in PREP activity<sup>41</sup> and neuronal cell loss, with concomitant loss of PREP expression.

Failure to correlate PREP activity (unchanged) and PREP expression (decreased) reflects a lack of understanding of the functioning of PREP in the brain. There is evidence



that PREP is involved in molecular interactions, eliciting an effect that is independent of its peptidase activity, but nevertheless may be modulated by inhibitor binding.<sup>22,38,42</sup> In addition to its involvement in neuroinflammation, PREP has been suggested to play a role in other neurodegenerative diseases and synaptic plasticity.<sup>14,17,23</sup> Furthermore, it has been frequently associated with secretion of neuropeptides and related to cognitive functions in the brain.<sup>43</sup> Because these pathologic and biochemical processes are highly relevant to the pathogenesis of TLE, it was reasonable to assume that inhibiting PREP would have beneficial effects by altering some of those functions following KASE induction in rats.

Despite a strong inhibition of PREP activity at 2 weeks in KASE animals following treatment, the neuroinflammatory response, cell loss, or cell proliferation remained unaltered. The 2-week timepoint evaluated in this study represented a period for which we have previously reported highest microglia activation, astrogliosis, and TSPO up-regulation.<sup>10</sup> Therefore, based on our hypothesis we expected a relation of PREP activity to neuroinflammation as well as a maximum response to PREP inhibition at this time point. Nevertheless, these results are in line with a recent finding from PREP<sup>-/-</sup> mice, where the absence of PREP did not change basal or post-LPS injection levels of proinflammatory cytokines.<sup>24</sup> As a limitation, our evaluations did not include levels of neuroinflammatory cytokines, but considering the published outcomes<sup>24</sup> we predict a similar result for expression of cytokines following PREP inhibition. Accordingly, we did not observe any temporal changes in the PREP activity during the progression of TLE from initial appearance of SRS (2-week time point) to development of a chronic epileptic condition when frequent SRS are observed. Moreover, no relation of PREP activity in the chronic epilepsy period was observed with the number of SRS/day, suggesting that PREP may not be associated with the appearance/progression of epileptic seizures in this model of TLE. Therefore, it was found not justifiable to study the effect of the PREP inhibitor on SRS or animal behavior over a prolonged period.

Despite our findings, we do not rule out the possibility that increasing PREP activity may alter pathologic outcomes in this model. However, considering that PREP activity did not change after 2 weeks in KASE animals, this is not likely.

In conclusion, contrary to previous reports, we found that PREP is not a direct mediator of neuroinflammatory glial activation, cell loss, and hippocampal subgranule zone cell proliferation, at least in the KASE model of epileptogenesis. It is also not altered during the period when chronic SRS are observed in this model. Taken together, these data show that inhibition of PREP may not have any beneficial effects on mitigating epileptogenesis or as an antiepileptic therapy.

## ACKNOWLEDGMENTS

This work was supported by a grant from the Research Foundation-Flanders (FWO #G038515N). We thank Timo Myöhänen for the anti-PREP antibody and Krystyna Szweczyk for her help in animal experiments.

## DISCLOSURE OF CONFLICTS OF INTEREST

None of the authors have potential conflicts of interest to disclose. We confirm that we have read the Journal's position on issues involved in ethical publication and affirm that this work is consistent with those guidelines.

## REFERENCES

1. Dedeurwaerdere S, Callaghan PD, Pham T, et al. PET imaging of brain inflammation during early epileptogenesis in a rat model of temporal lobe epilepsy. *EJNMMI Res* 2012;2:60.
2. Maroso M, Balosso S, Ravizza T, et al. Toll-like receptor 4 and high-mobility group box-1 are involved in ictogenesis and can be targeted to reduce seizures. *Nat Med* 2010;16:413–419.
3. Ali I, Chugh D, Ekdahl CT. Role of fractalkine-CX3CR1 pathway in seizure-induced microglial activation, neurodegeneration, and neuroblast production in the adult rat brain. *Neurobiol Dis* 2015;74:194–203.
4. Ulmann L, Levavasseur F, Avignone E, et al. Involvement of P2X4 receptors in hippocampal microglial activation after status epilepticus. *Glia* 2013;61:1306–1319.
5. Kawasaki Y, Zhang L, Cheng JK, Ji RR. Cytokine mechanisms of central sensitization: distinct and overlapping role of interleukin-1beta, interleukin-6, and tumor necrosis factor-alpha in regulating synaptic and neuronal activity in the superficial spinal cord. *J Neurosci* 2008;28:5189–5194.
6. Vezzani A, Viviani B. Neuromodulatory properties of inflammatory cytokines and their impact on neuronal excitability. *Neuropharmacology* 2015;96:70–82.
7. Chugh D, Ali I, Bakochi A, Bahonjic E, Etholm L, Ekdahl CT. Alterations in brain inflammation, synaptic proteins, and adult hippocampal neurogenesis during epileptogenesis in mice lacking synapsin2. *PLoS ONE* 2015;10:e0132366.
8. Ekdahl CT, Claasen JH, Bonde S, Kokaia Z, Lindvall O. Inflammation is detrimental for neurogenesis in adult brain. *Proc Natl Acad Sci* 2003;100:13632–13637.
9. Amhaoul H, Ali I, Mola M, et al. P2X7 receptor antagonism reduces the severity of spontaneous seizures in a chronic model of temporal lobe epilepsy. *Neuropharmacology* 2016;105:175–185.
10. Amhaoul H, Hamaide J, Bertoglio D, et al. Brain inflammation in a chronic epilepsy model: evolving pattern of the translocator protein during epileptogenesis. *Neurobiol Dis* 2015;82:526–539.
11. Semple BD, O'Brien TJ, Gimlin K, et al. Interleukin-1 receptor in seizure susceptibility after traumatic injury to the pediatric brain. *J Neurosci* 2017;37:7864–7877.
12. Pauletti A, Terrone G, Shekh-Ahmad T, et al. Targeting oxidative stress improves disease outcomes in a rat model of acquired epilepsy. *Brain* 2017;140:1885–1899.

13. Penttinen A, Tenorio-Laranga J, Siikanen A, et al. Prolyl oligopeptidase: a rising star on the stage of neuroinflammation research. *CNS Neurol Disord Drug Targets* 2011;10:340–348.
14. Moreno-Baylach MJ, Felipo V, Mannisto PT, Garcia-Horsman JA. Expression and traffic of cellular prolyl oligopeptidase are regulated during cerebellar granule cell differentiation, maturation, and aging. *Neuroscience* 2008;156:580–585.
15. Moreno-Baylach MJ, Puttonen KA, Tenorio-Laranga J, et al. Prolyl endopeptidase is involved in cellular signalling in human neuroblastoma SH-SY5Y cells. *Neurosignals* 2011;19:97–109.
16. Morawski M, Schulz I, Zeitschel U, Blossa M, Seeger G, Rossner S. Role of prolyl endopeptidase in intracellular transport and protein secretion. *CNS Neurol Disord Drug Targets* 2011;10:327–332.
17. Hannula MJ, Myohanen TT, Tenorio-Laranga J, Mannisto PT, Garcia-Horsman JA. Prolyl oligopeptidase colocalizes with alpha-synuclein, beta-amyloid, tau protein and astroglia in the post-mortem brain samples with Parkinson's and Alzheimer's diseases. *Neuroscience* 2013;242:140–150.
18. Klegeris A, Li J, Bammler TK, et al. Prolyl endopeptidase is revealed following SILAC analysis to be a novel mediator of human microglial and THP-1 cell neurotoxicity. *Glia* 2008;56:675–685.
19. Tenorio-Laranga J, Montoliu C, Urios A, et al. The expression levels of prolyl oligopeptidase responds not only to neuroinflammation but also to systemic inflammation upon liver failure in rat models and cirrhotic patients. *J Neuroinflammation* 2015;12:183.
20. O'Reilly PJ, Hardison MT, Jackson PL, et al. Neutrophils contain prolyl endopeptidase and generate the chemotactic peptide, PGP, from collagen. *J Neuroimmunol* 2009;217:51–54.
21. Benson MJ, Manzanero S, Borges K. The effects of C5aR1 on leukocyte infiltration following pilocarpine-induced status epilepticus. *Epilepsia* 2017;58:e54–e58.
22. Di Daniel E, Glover CP, Grot E, et al. Prolyl oligopeptidase binds to GAP-43 and functions without its peptidase activity. *Mol Cell Neurosci* 2009;41:373–382.
23. D'Agostino G, Kim JD, Liu ZW, et al. Prolyl endopeptidase-deficient mice have reduced synaptic spine density in the CA1 region of the hippocampus, impaired LTP, and spatial learning and memory. *Cereb Cortex* 2013;23:2007–2014.
24. Hofling C, Kuleshkaya N, Jaako K, et al. Deficiency of prolyl oligopeptidase in mice disturbs synaptic plasticity and reduces anxiety-like behaviour, body weight, and brain volume. *Eur Neuropsychopharmacol* 2016;26:1048–1061.
25. Jaako K, Waniek A, Parik K, et al. Prolyl endopeptidase is involved in the degradation of neural cell adhesion molecules in vitro. *J Cell Sci* 2016;129:3792–3802.
26. Bonfanti L. PSA-NCAM in mammalian structural plasticity and neurogenesis. *Prog Neurobiol* 2006;80:129–164.
27. Pekcec A, Muhlenhoff M, Gerardy-Schahn R, Potschka H. Impact of the PSA-NCAM system on pathophysiology in a chronic rodent model of temporal lobe epilepsy. *Neurobiol Dis* 2007;27:54–66.
28. Ahmed MM, Arif M, Chikuma T, Kato T. Pentylentetrazol-induced seizures affect the levels of prolyl oligopeptidase, thimet oligopeptidase and glial proteins in rat brain regions, and attenuation by MK-801 pretreatment. *Neurochem Int* 2005;47:248–259.
29. Jarho EM, Venalainen JJ, Huuskonen J, et al. A cyclorent-2-enecarbonyl group mimics proline at the P2 position of prolyl oligopeptidase inhibitors. *J Med Chem* 2004;47:5605–5607.
30. Jalkanen AJ, Hakkarainen JJ, Lehtonen M, et al. Brain pharmacokinetics of two prolyl oligopeptidase inhibitors, JTP-4819 and KYP-2047, in the rat. *Basic Clin Pharmacol Toxicol* 2011;109:443–451.
31. Hellier JL, Patrylo PR, Buckmaster PS, Dudek FE. Recurrent spontaneous motor seizures after repeated low-dose systemic treatment with kainate: assessment of a rat model of temporal lobe epilepsy. *Epilepsy Res* 1998;31:73–84.
32. van Raay L, Morris MJ, Reed RC, O'Brien TJ, Dedeurwaerdere S. A novel system allowing long-term simultaneous video-electroencephalography recording, drug infusion and blood sampling in rats. *J Neurosci Methods* 2009;179:184–190.
33. Paxinos G, Watson C. *The rat brain in stereotaxic coordinates*. 6th ed. Amsterdam: Elsevier Academic Press; 2007.
34. Bertoglio D, Amhaoul H, Van Eetveldt A, et al. Kainic acid-induced post-status epilepticus models of temporal lobe epilepsy with diverging seizure phenotype and neuropathology. *Front Neurol* 2017;8:588.
35. Sharma AK, Jordan WH, Reams RY, Hall DG, Snyder PW. Temporal profile of clinical signs and histopathologic changes in an F-344 rat model of kainic acid-induced mesial temporal lobe epilepsy. *Toxicol Pathol* 2008;36:932–943.
36. Tedesco V, Ravagnani C, Bertoglio D, Chiamulera C. Acute ketamine-induced neuroplasticity: ribosomal protein S6 phosphorylation expression in drug addiction-related rat brain areas. *NeuroReport* 2013;24:388–393.
37. Van den Eynde K, Missault S, Fransen E, et al. Hypolocomotive behaviour associated with increased microglia in a prenatal immune activation model with relevance to schizophrenia. *Behav Brain Res* 2014;258:179–186.
38. Brandt I, Gerard M, Sergeant K, et al. Prolyl oligopeptidase stimulates the aggregation of alpha-synuclein. *Peptides* 2008;29:1472–1478.
39. Julku UH, Panhelainen AE, Tiilikainen SE, et al. Prolyl oligopeptidase regulates dopamine transporter phosphorylation in the nigrostriatal pathway of mouse. *Mol Neurobiol* 2018;55:470–482.
40. Jalkanen AJ, Piepponen TP, Hakkarainen JJ, et al. The effect of prolyl oligopeptidase inhibition on extracellular acetylcholine and dopamine levels in the rat striatum. *Neurochem Int* 2012;60:301–309.
41. Arif M, Chikuma T, Ahmed MM, Nakazato M, Smith MA, Kato T. Effects of memantine on soluble Alpha(25-35)-induced changes in peptidergic and glial cells in Alzheimer's disease model rat brain regions. *Neuroscience* 2009;164:1199–1209.
42. Savolainen MH, Yan X, Myohanen TT, Huttunen HJ. Prolyl oligopeptidase enhances alpha-synuclein dimerization via direct protein-protein interaction. *J Biol Chem* 2015;290:5117–5126.
43. Babkova K, Korabecny J, Soukup O, et al. Prolyl oligopeptidase and its role in the organism: attention to the most promising and clinically relevant inhibitors. *Future Med Chem* 2017;9:1015–1038.

**How to cite this article:** Ali I, Van Eetveldt A, Van Elzen R, et al. Spatiotemporal expression and inhibition of prolyl oligopeptidase contradict its involvement in key pathologic mechanisms of kainic acid-induced temporal lobe epilepsy in rats. *Epilepsia Open*. 2019;4:92–101. <https://doi.org/10.1002/epi4.12293>